The "Hockey Sticks" Effect Revisited: The Conformational and Electronic Properties of 3,7-Dithia-1,5-diazabicyclo[3.3.1]nonane from the QTAIM Perspective

ARTICLE *in* THE JOURNAL OF PHYSICAL CHEMISTRY A · SEPTEMBER 2011

Impact Factor: 2.69 · DOI: 10.1021/jp203730b · Source: PubMed

8 AUTHORS, INCLUDING:

Ivan Bushmarinov
Russian Academy of Sciences
84 PUBLICATIONS **322** CITATIONS
SEE PROFILE

Konstantin A Lyssenko
Russian Academy of Sciences
761 PUBLICATIONS **6,110** CITATIONS
SEE PROFILE

Nikolai S Zefirov
Tufts Medical Center
1,141 PUBLICATIONS **7,134** CITATIONS
SEE PROFILE

THE JOURNAL OF PHYSICAL CHEMISTRY A

ARTICLE

pubs.acs.org/JPCA

The "Hockey Sticks" Effect Revisited: The Conformational and Electronic Properties of 3,7-Dithia-1,5-diazabicyclo[3.3.1]nonane from the QTAIM Perspective

I. S. Bushmarinov,[†] I. V. Fedyanin,[†] K. A. Lyssenko,[*,†] V. L. Lapteva,[‡] S. A. Pisarev,[§] V. A. Palyulin,[‡] N. S. Zefirov,[‡] and M. Yu. Antipin[†]

[†]A.N. Nesmeyanov Institute of Organoelement Compounds, Russian Academy of Sciences, Vavilova Str., 28, 119991 Moscow, Russia

[‡]Department of Chemistry, Moscow State University, Leninskie gory, 1/3, Moscow 119991 Russia

[§]Institute of Physiologically Active Compounds, Russian Academy of Sciences, Severny proezd, 1, Chernogolovka, Moscow region, 142432, Russia

Supporting Information

ABSTRACT: The conformational effects in bicyclo[3.3.1]nonanes, while thoroughly studied, have not yet received the full theoretical explanation. R. F. W. Bader's quantum theory of atoms in molecules presents unique opportunities for studying the stereoelectronic interactions (SEI) and weak intramolecular bonding leading to these effects. Here, we report the study of 3,7-dithia-1,5-diazabicyclo[3.3.1]nonane by means of the topological analysis of the calculated (MP2(full)/6-311++G**) and experimental (X-ray derived) charge density to reveal the origins of the so-called "hockey sticks" effect observed in similar compounds. A new explanation of the relative stability of bicyclo[3.3.1]nonane conformers based on the analysis of the QTAIM atomic energies is given. The H···H and S···S interactions in bicyclo-[3.3.1]nonane and its dithia derivatives are shown to be significant factors contributing to the differences in the relative stability of the conformers.

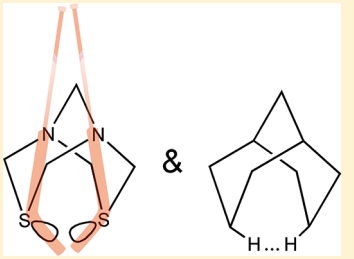

INTRODUCTION

R. F. W. Bader's quantum theory of atoms in molecules has given a definition of an atom as a region in real space bounded by a zero-flux surface, for which all the properties computable for a molecule and defined locally can be calculated.[1] The concept of transferability accompanying this definition states that two identical atoms in two different molecules should have identical properties.[2,3] The transferability within the limits of chemical accuracy (with the difference between the compared groups not exceeding 1 kcal/mol in energy and 0.001 e in electronic population) is of rare occurrence "in the face of unavoidable perturbations induced in the groups by their transfer between molecules".[4] It is still possible, however, to compare properties of individual atoms belonging to different molecules, since the changes in atomic properties are usually accompanied by opposite changes for the neighboring atoms, causing the properties of the molecule as a whole to persist—the effect is called "compensatory transferability".[4] The applicability of such comparisons has been proved in the case of hydrocarbon compounds, and the comparative analysis of atoms' energies has been used to investigate the sources of the strain in cycloalkanes.[2,5] Further progress in the comparative analysis of atomic electronic populations and energies offered deeper insights into the nature and energy of intra- and intermolecular interactions. One of the most notable results obtained by such approach is the classification of various hydrogen bonding interactions, including weak ones such as C−H···O[6] and H···H,[7,8] but it has been shown to be a useful tool for the conformational analysis as well.[9−11] In our recent charge density studies,[12,13] the same approach has been successfully applied to explore the LP−X−C−Y (where X and Y are heteroatoms and LP is a lone pair) stereoelectronic interactions (further SEI) in various systems. It has been shown that such interactions, which usually lead to an increase in the relative stability of the conformation with the antiperiplanar disposition of a lone pair and a polar bond (the so-called generalized anomeric effect,[14] Scheme 1), are accompanied by a decrease in energy and increase of electronic populations of the atoms X and Y and comparable opposite changes of both for the atom C.[12]

The changes in energies of the atoms X, Y, and C have been shown to be more pronounced for stronger SEI that allows for direct comparison of effects of SEI on individual atoms with contributions from other intra- and intermolecular interactions. In particular, this approach has been successfully used to separate the contributions of SEI and those of the destabilizing effect caused by the proximity of lone pairs of nitrogen atoms in the molecule of tetrahydro-[1,3,4]thiadiazolo[3,4-*c*][1,3,4]thiadiazole[12]

Special Issue: Richard F. W. Bader Festschrift

Received: April 21, 2011
Revised: August 8, 2011

Scheme 1. The Generalized Anomeric Effect

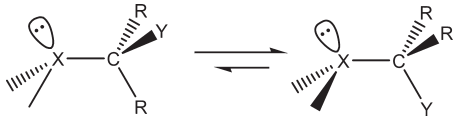

(**TDZTDZ**) and to compare the effects of SEI and Cl···O_2N interactions in substituted aziridines.[13]

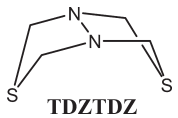

TDZTDZ

As the QTAIM theory requires only the electron density distribution function $\rho(\mathbf{r})$ for the topological analysis and the local energy density can be estimated from $\rho(\mathbf{r})$, the same technique was applied to the $\rho(\mathbf{r})$ functions obtained from quantum chemical calculations and multipole refinement of high-resolution single-crystal X-ray diffraction (XRD) data, giving consistent results not only for the variation of atomic electronic populations but even for the atomic energies.[12]

The use of the QTAIM theory is also a rigorous way to identify and classify all attractive interactions within the studied system, including weak and possibly unexpected ones like H···H.[15,16] Within the QTAIM theory, any bonding interaction is manifested in $\rho(\mathbf{r})$ as a (3,−1) critical point (usually abbreviated as BCP, from "bond critical point") and a gradient path (the so-called "bond path") linking two interacting atoms. The values of $\rho(\mathbf{r})$, $-\nabla^2\rho(\mathbf{r})$, and other properties at this BCP produce significant information on the strength and nature of the studied interaction.[1] Furthermore, the application of the correlation proposed by Espinosa et al.[17−21] (CEML), which interconnects the energy of an interaction (E_{int}) with the potential energy density $v(\mathbf{r})$ in its BCP, allows estimating the energy of various interactions;[22−27] their examples being Mg···C and Ca···C coordinate bonds in zeolite inclusion complexes[28,29] (DFT studies), Si−N bonds in hypervalent silicon compounds,[30] Gd−OH_2, Gd−N(phenanthroline), Gd−Cl,[31] and Au−P[32] bonds (XRD data). The accuracy of the results obtained by this approach for various weak interactions was unambiguously demonstrated by comparing the crystal lattice energy estimated within CEML and the experimental sublimation enthalpy;[23−27] it was also used for the estimation of energetic characteristics of the pseudosymmetry phenomenon[33] and for the comparison of polymorphic modifications.[27]

To continue our study of the LP−N−C−S systems, we have chosen the 3,7-dithia-1,5-diazabicyclo[3.3.1]nonane (**DTDABCN**) as the next target for the QTAIM-assisted conformational analysis based on the topological analysis of both the experimental and theoretical $\rho(\mathbf{r})$ functions. In addition, as the atomic energies in the bicyclo[3.3.1]nonane system have been never studied before, we aimed to evaluate the origins of conformational preferences in unsubstituted bicyclo[3.3.1]nonane using the same approach. The molecule of **DTDABCN** demonstrates an unusual stabilization of the *cc* conformation that can be attributed to the attractive S···S interaction, and the conformation preferences in the bicyclo[3.3.1]nonane system are particularly susceptible to weak intramolecular interactions. In particular, as it has been previously shown, the weak intramolecular B···π bonding can stabilize the extremely unusual chair−chair conformation of 7α-phenyl-3-borabicyclo[3.3.1]nonanes.[34,35]

Scheme 2. The "Hockey Sticks" Effect

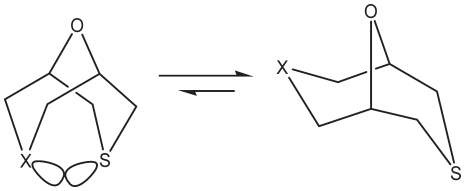

X= S, Se

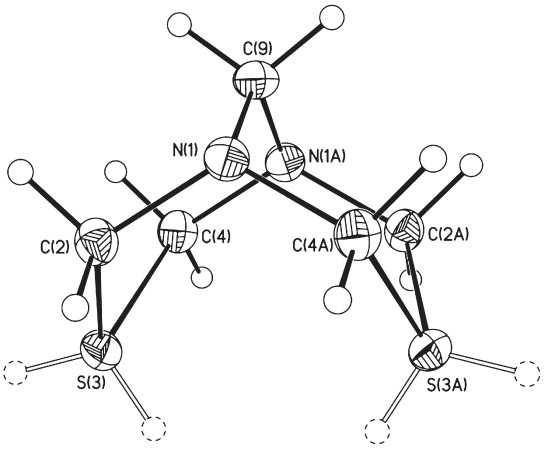

Figure 1. The general view of **DTDABCN** in a crystal. The molecule is lying around a C_2 axis passing through the C(9) atom. Atoms are represented by thermal displacement ellipsoids (p = 50%); symmetry-equivalent atoms have postfix "A", and theoretical positions of sulfur LPs are denoted by dashed circles.

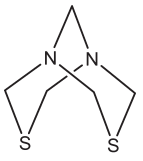

DTDABCN

RESULTS AND DISCUSSION

The conformational properties of bicyclo[3.3.1]nonane derivatives have been studied for a long time, and they can be predicted with high accuracy by quantum chemical calculations. These systems cannot be called conformationally rich, as they typically feature only two principal conformations: chair−chair (further *cc*) and chair−boat (further *cb*). At the same time, the origins of the conformational preferences of such rigid systems have been thoroughly studied, and most of the experimental and computational data available for bicyclo[3.3.1]nonane can be explained in simple terms of "repulsion of substituents" and "repulsive interaction of heteroatomic lone pairs".[36,37] One of such examples is the so-called "hockey sticks" effect:[38] an unusual conformational preference of the 9-oxa-3,7-dithiabicyclo[3.3.1]-nonane as well as 9-oxa-3-selena-7-thiabicyclo[3.3.1]nonane

dx.doi.org/10.1021/jp203730b |J. Phys. Chem. A XXXX, XXX, 000–000

leading to the *cb* conformation, while the similar 3-thia-7-oxa compounds display no such preference and favor the *cc* conformation[39,40] (Scheme 2). This effect was explained by the repulsion of LPs of the bulky atoms of sulfur and/or selenium. The **DTDABCN**, however, seems to be an exception: the crystallographic data[41−43] show that the molecule is in the *cc* conformation (Figure 1). The aim of the current study is to analyze the different contributions to the relative stability of the conformers of 3,7-dithia-1,5-diazabicyclo[3.3.1]nonane and related molecules and, in particular, to estimate the role of intramolecular S···S interaction and LP−N−C−S SEI in it.

The molecular geometry of **DTDABCN** in a crystal indicates the presence of a strong LP−N−C−S SEI: the nitrogens' LPs are antiperiplanar to the C−S bonds, the C−S bonds are elongated by 0.03 Å from the CSD typical value,[44] and the C−N ones are shortened by 0.02 Å (Table 1). Such changes in bond lengths are typical geometrical evidence of a SEI.[14]

The topological analysis of the experimental $\rho(\mathbf{r})$function for **DTDABCN** has found the BCPs for all the covalent bonds as well as for some closed-shell[45] interactions: the intramolecular S(3)···S(3A) (d = 3.366(1) Å) and intermolecular S···H and H···H ones. The E_{int} for these interactions was estimated as 3 kcal/mol for the intramolecular S···S and as 0.6—1.6 kcal/mol for the intermolecular interactions (see Supporting Information, Tables S1 and S2). The electron density parameters at the BCP for the S···S interaction ($\rho(\mathbf{r})$ = 0.11 e·Å^{-3}, $-\nabla^2\rho(\mathbf{r})$ = 1.02 e·Å^{-5}, see Table 2) show that it is significantly stronger than the previously reported intermolecular S···S interactions.[12,46] Two symmetrically equivalent CPs (3,+1) corresponding to the S(3)−C(2)−N(1)−C(4A)−S(3A) cycles were also found, and the distance from each of them to the S···S BCP is 0.48 Å, indicative of a stable molecular graph.

The deformation electron density (DED) (Figure 2) and $-\nabla^2\rho(\mathbf{r})$ (Figure 3) maps in the S(3)−C(9)−S(3A) plane of **DTDABCN** show that the S···S interaction is of the "peak-to-peak" type. In the DED map the "endo" (pointing inward) LP of the S(3) atom is apparently bigger than the "exo" one. The $-\nabla^2\rho(\mathbf{r})$ map, however, does not indicate any visible difference between these lone pairs. Indeed, the topological analysis of

Table 1. The Selected Bond Lengths (Å) of DTDABCN in a Crystal and Its Conformers in an Isolated State According to the MP2 Calculation, Compared with the Typical Values of C(sp^3)−S(sp^3) and C(sp^3)−N(sp^3) Bond Lengths

bond	DTDABCN	SN-cc	SN-cb	typical value[44]
N(1)−C(2)	1.4497(7)	1.446	1.447	1.469
	1.4461(8)			
N(1)−C(8)			1.477	1.469
C(2)−S(3)	1.8484(6)	1.846	1.845	1.814
	1.8518(6)			
C(8)−S(7)			1.818	1.814
N(1)−C(9)	1.4600(6)	1.454	1.459	1.469
S(3)···S(7)	3.3659(3)	3.377		

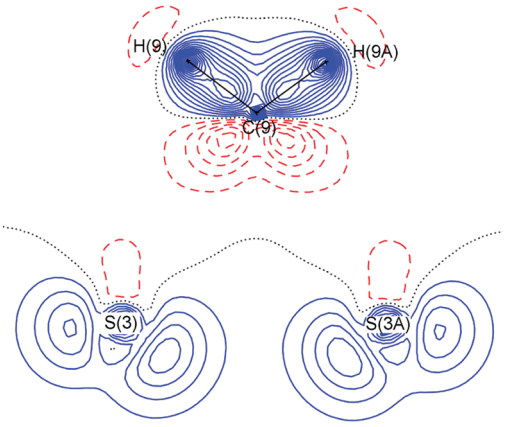

Figure 2. The deformation electron density (DED) contour map for the S(3)−C(9)−S(3A) plane in a crystal of **DTDABCN** with a step of 0.05 e·Å^{-3}. The red dashed lines denote the negative values, the blue solid lines denote the positive values, and the black dotted line denotes the zero contour. The DED function $\delta\rho(\mathbf{r}) = \rho(\mathbf{r}) - \tilde{\rho}(\mathbf{r})$ represents the difference between the electron density of the system, $\tilde{\rho}$, and the electron density of a set of spherically averaged noninteracting atoms, ρ, placed at the same positions as the atoms of the system.

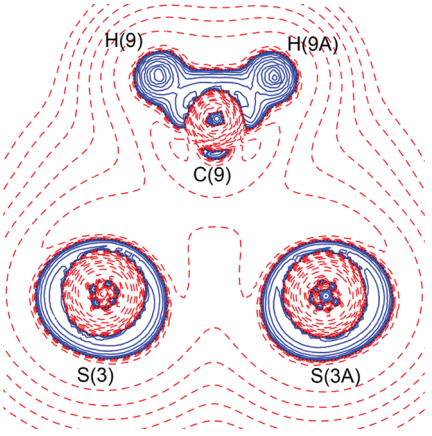

Figure 3. The experimental $-\nabla^2\rho(\mathbf{r})$ map for the S(3)−C(9)−S(3A) plane in a crystal of **DTDABCN** with the contour values of $\pm 0.05 \cdot 2^n$ e·Å^{-5}, $n \in \{1, ..., 30\}$. The red dashed lines denote the negative values; the blue solid lines denote the positive values.

Table 2. The Distances, Delocalization Indices (DI), and Topological Properties of Electron Density Functions at BCPs Corresponding to Interactions between Sulfur Atoms or CH_2 Groups in 3,7 Positions in DTDABCN and Its Derivatives in a Crystal and in an Isolated State[a]

compound	interaction	d, Å	$\rho(\mathbf{r})$, e·Å^{-3}	$-\nabla^2\rho(\mathbf{r})$, e·Å^{-5}	ε	$v(\mathbf{r})$, au	DI	E_{int}, kcal/mol
DTDABCN	S(3)···S(3A)	3.3659(3)	0.11	1.02	0.19	−0.010		3.09
SN-cc	S(3)···S(3A)	3.377	0.09	0.89	0.03	−0.008	0.104	2.64
SC-cc	S(3)···S(3A)	3.379	0.09	0.91	0.06	−0.008	0.098	2.60
CC-cc	H(3A)···H(3AA)	1.910	0.10	1.23	0.29	−0.009	0.038	2.93

[a] Labels are defined in Figure 4.

dx.doi.org/10.1021/jp203730b |J. Phys. Chem. A XXXX, XXX, 000–000

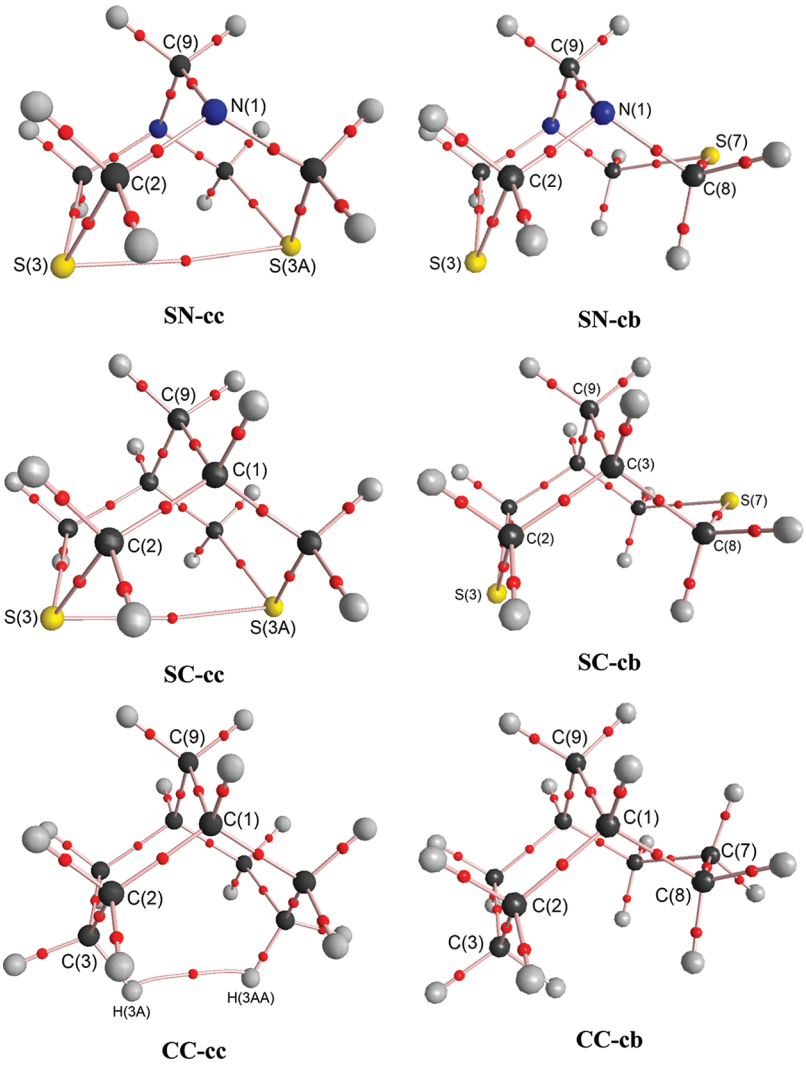

Figure 4. The molecular graphs of the calculated conformers of **DTDABCN** and its derivatives in an isolated state. Only symmetrically independent atoms and/or atoms participating in the 3,7 interaction are labeled. (3,−1) critical points are shown in red, (3,+1) and (3,+3) ones are omitted for clarity.

$-\nabla^2\rho(\mathbf{r})$ shows that the (3,−3) CPs corresponding to these lone pairs are very similar: the $\rho(\mathbf{r})$, $-\nabla^2\rho(\mathbf{r})$, and r (where r corresponds to the distance to the atom nucleus) values at these points differ by less than 3%, the maximum being the difference in the $\rho(\mathbf{r})$ (Table 4). The values of all these parameters are, however, higher (by absolute value) for the "endo" CP, and it is likely that the accumulation of electron density on the "endo" sulfur LP is caused by the bonding S···S interaction. This means that the studied interaction is substantially different from the typical S···S ones, which usually occur by the "peak-to-hole" mechanism.[47,48] The bonding interaction of the "peak-to-peak" type, however, can be observed, as, e.g., the $Cl^-\cdots Cl^-$ shortened contact in the crystalline hydroxylammonium chloride.[49] Moreover, a very similar interaction with the energy of 1.7 kcal/mol and the S···S distance of 3.223 Å was observed in the theoretically modeled endo-envelope−envelope conformation of TDZTDZ.[12]

Such an interaction could affect the strength of the LP−N−C−S SEI in **DTDABCN**, but the amount and even the "sign" of its impact could not be judged using the experimental $\rho(\mathbf{r})$ function, as only one possible conformer is observed in a crystal.

Further analysis of the **DTDABCN** conformational preferences required a quantum chemical calculation of its *cc* and *cb* conformers in an isolated state (further **SN-cc** and **SN-cb**, respectively) (Figure 4). In addition, as the different behavior was expected for the conformer without the possibility to form an LP−N−C−S SEI, we have chosen the 3,7-dithiabicyclo-[3.3.1]nonane as a model compound to evaluate the "pure" "hockey sticks" effect without the LP−N−C−S SEI contribution (conformers **SC-cc** and **SC-cb**) (Figure 4). Bicyclo-[3.3.1]nonane was chosen as a reference molecule with neither SEI nor the "hockey sticks" effect affecting its conformational preferences (conformers **CC-cc** and **CC-cb**) (Figure 4).

The calculations for all the above conformers were performed at the MP2(full)/6-311++G** level of theory (see Computational Details). It is noteworthy that the calculated geometry of the **SN-cc** conformer is very close to the experimental one: the differences in bond lengths do not exceed 0.005 Å (Table 1).

The *cc* conformation of **DTDABCN** observed in a crystal is also the most favorable in an isolated state. At the same time, the more favorable conformation of the **SC** derivative is *cb*, following

dx.doi.org/10.1021/jp203730b |*J. Phys. Chem. A* XXXX, XXX, 000–000

Table 3. The Energetic and Strain Characteristics of the Conformers of DTDABCN and Its Analogues (see Figure 4), According to the MP2 Calculation with ZPE Correction[a]

	SN-cb	SN-cc	SC-cb	SC-cc	CC-cb	CC-cc
E, hartree	−1100.9057	−1100.9117	−1068.8873	−1068.8850	−351.7412	−351.7451
$E(cc) - E(cb)$, kcal/mol		−3.80		1.43		−2.46
$\Sigma\lvert\Delta\alpha\rvert$, deg	64.6	60.9	33.6	34.4	18.4	22.3
$(\Sigma\lvert\Delta\alpha\rvert)_{cc} - (\Sigma\lvert\Delta\alpha\rvert)_{cb}$, deg		−3.7		0.8		3.9

[a] $\Delta\alpha$ denotes the difference between geometric bond angle and bond path angle, and the summation is performed over all bond angles formed by shared interactions not involving hydrogens.

Table 4. The Selected Properties of $-\nabla^2\rho(\mathbf{r})$ at CPs (3,−3) Corresponding to the LP of the S(3) Atom in a Crystal of DTDABCN and in the Calculated Conformers SN-cc and SN-cb

	DTDABCN (crystal)		SN-cc		SN-cb	
	endo	exo	endo	exo	endo	exo
r, Å	0.696	0.696	0.688	0.690	0.690	0.691
$\rho(\mathbf{r})$, e·Å^{-3}	1.30	1.27	1.34	1.32	1.32	1.30
$-\nabla^2\rho(\mathbf{r})$, e·Å^{-5}	−11.99	−11.93	−13.97	−13.50	−13.57	−13.08

Table 5. The Changes in Integral Energies (E) and Electronic Populations (N) of Symmetrically Independent Groups (and/or atoms) in the Conformers and the Derivatives of DTDABCN in an Isolated State upon the Transition from the *cb* Conformation to *cc* (see Figure 4)

	ΔE, kcal/mol			ΔN, e		
	SN	SC	CC	SN	SC	CC
N(1)	−34.9			0.036		
C(1)H		−4.0	−4.6		−0.009	−0.006
C(2)H_2	9.7	3.4	4.3	−0.006	0.003	0.003
S(3)	2.1	2.2		−0.031	−0.017	
C(3)H_2			−1.6			−0.002
C(6)H_2	26.7	0.0	1.9	−0.058	0.008	−0.001
S(7)	−18.2	−3.4		0.075	−0.010	
C(7)H_2			−5.4			0.007
C(9)H_2	8.4	3.8	1.5	0.006	0.019	0.006

the tendency expected for the "hockey sticks" effect (see Scheme 2). The difference in energy (with ZPE correction) between the bicyclo[3.3.1]nonane conformers **CC-cc** and **CC-cb** agrees well with the results of the gas-phase electron diffraction thermochemical studies that estimated the corresponding ΔH as 2.5 kcal/mol.[50]

The topological properties of both the $\rho(\mathbf{r})$ and $-\nabla^2\rho(\mathbf{r})$ functions for **SN-cc** showed a very good agreement with the experimental ones for **DTDABCN**. The molecular graph of **SN-cc** is identical to that of **DTDABCN**, and the values of $\rho(\mathbf{r})$ at BCPs of C−S and C−N bonds, as well as the characteristics of the S···S interaction ($\rho(\mathbf{r})$= 0.09 e·Å^{-3}, $-\nabla^2\rho(\mathbf{r})$ = 0.89 e·Å^{-5}, E_{int} = 3.1 kcal/mol) (see Table 2), are very close to that, observed in a crystal. The topology of $-\nabla^2\rho(\mathbf{r})$ in the vicinity of this interaction was reproduced even better (see Table 4), showing the same tendencies in the properties of $-\nabla^2\rho(\mathbf{r})$ CPs (3,−3).

The chair−boat conformation of **SN-cb** excludes the presence of the LP−N−C−S SEI involving the S(7) atom. As a consequence, the C(8)−S(7) bond in **SN-cb** is 0.03 Å shorter than the C(2)−S(3) one, and the N(1)−C(8) bond is 0.03 Å longer than the N(1)−C(2) one (see Table 1). The properties of the $-\nabla^2\rho(\mathbf{r})$ at CPs(3,−3) corresponding to the lone pairs of sulfur atoms also show that the difference between "endo" and "exo" lone pairs remains the same in the absence of the S···S interaction and thus is not caused by the latter. The fact that the difference between LPs is not lower in the *cc* conformation can be, however, attributed to the S···S interaction accompanied by the accumulation of the electron density between the sulfur atoms despite the proximity of their lone pairs.

The **SC-cc** and **CC-cc** conformers also featured the bonding interactions between the atoms occupying the positions 3 and 7 of the bicyclo[3.3.1]nonane skeleton. These interactions are summarized in Table 2. All the properties of S···S interactions in the **SN-cc** and **SC-cc** conformers are almost identical, clearly indicating that this interaction is not interfering with the LP−N−C−S SEI.

The relatively strong H···H bonding (E_{int} = 2.93 kcal/mol) in the **CC-cc** conformer is also of interest, as the presence of an attractive H···H interaction in bicyclo[3.3.1]nonane has not been even suggested in the literature. Although its delocalization index is lower than that for the S···S interaction, it resulted from the hydrogens having fewer electrons than the sulfur atoms to delocalize. The topological parameters at the corresponding BCP and the E_{int} value indicate that this interaction is very similar to the S···S one and should lead to the same stabilization. This conclusion, however, raises the question: how is it that we can explain the fact that while the bicyclo[3.3.1]nonane prefers the *cc* conformation, the same *cc* conformation of its 3,7-dithia derivative featuring a very similar 3,7 attractive interaction is less stable than the *cb* one?

We can answer this question by analyzing the variations of the atomic energy and electronic populations in the calculated conformers upon the transition from the *cb* to the *cc* conformation (Table 5); the CH− and CH_2− fragments were treated as a whole to simplify the discussion of the observed variations (the compared values can be found in Table S3, Supporting Information). The integral Lagrangian values of the individual atoms being less than 2×10^{-3} au and the charge leakage less than 5×10^{-3} e for all the calculated conformers (see Tables S10−S15, Supporting Information) ensured the reliability of the results obtained. The differences in virial ratios of compared conformers were low enough to compare the scaled atomic energies directly (see Table S16, Supporting Information).

dx.doi.org/10.1021/jp203730b |J. Phys. Chem. A XXXX, XXX, 000–000

Note that the changes for the **SN** conformers upon the transition are the most dramatic ones (up to $\Delta E = -34.6$ kcal/mol and $\Delta N = 0.036$ e) and are mostly caused by the LP−N−C−S SEI. Indeed, the electron populations of the nitrogen atoms become higher by 0.036 e, the S(7) electronic population increases by 0.075 e, the electronic populations of the neighboring carbons decrease, and the changes in energy correlate with the changes in electronic populations; this pattern is similar to one previously reported for the LP−N−C−S SEI in TDZTDZ.[12]

The differences between the **SN** conformers are therefore in line with predictions based on the LP−N−C−S anomeric effect. The differences in relative stablility of **SC** and **CC** conformers, however, remain unexplained. The estimation of strain in these compounds can be obtained from the values of difference between geometric bond angle and bond path angle ($\Delta\alpha$), as proposed by Bader and Wiberg.[51] The more pronounced these deviations are, the higher is the estimated strain in the molecule. The values of $\Delta\alpha$ for all shared interactions not involving hydrogens in studied conformers can be found in Tables S22−S25 in the Supporting Information, and the sums of their absolute values are listed in Table 4. The values for the **SN** conformers are mostly defined by the changes in $\Delta\alpha_{C-N}$ resulting from the SEIs. The values of $\Sigma|\Delta\alpha|$ indicate that the strain in the *cb* conformers of **SN** and **SC** is actually lower than the strain in *cc* conformers. Moreover, the buildup of strain upon the transition from *cb* to *cc* is higher in the **CC** conformers. This is in line with the results of the strain energy calculations for cyclohexane and thiopyran, where the sulfur-containing compound is characterized by lesser strain and lesser difference in the strain of the *boat* structure compared to the *chair* (for the corresponding hyperhomodesmotic reaction scheme and details of these calculations see Computational Details below).

Thus, the discrepancy in $E(cc) - E(cb)$ between **SC** and **CC** can be explained only by the differences in the 3,7 interactions between **SC-cc** and **CC-cc**. These interactions have similar topological properties (see Table 2); thus the nature, and not strength, of these contacts must be different to explain the observed discrepancies. Indeed, the transition from **SC-cb** to **SC-cc** is accompanied by the decrease in electronic populations of the S(3) and S(7) atoms and the increase of energy for S(3), which is a typical example of the destabilization due to the heteroatomic LPs approaching each other (see, e.g., ref [9]). The unsubstituted bicyclo[3.3.1]nonane demonstrates the opposite tendency: the transition from **CC-cb** to **CC-cc** does not result in the decrease in electronic populations of the $C(3)H_2$ and $C(7)H_2$ groups. The energy of the $C(3)H_2$ group even becomes lower by 1.6 kcal/mol. Thus, the approach of H atoms by 1.91 Å is more favorable than the approach of S atoms by 3.379 Å, this difference is manifested in the energies of participating atoms and defines the conformational preferences of bicyclo[3.3.1]nonane and its 3,7-dithia derivative.

The effects mentioned above can be semiquantitatively estimated as follows. We can suggest two main factors underlying the variations of the atomic energies upon the transition from **CC-cb** to **CC-cc**: (i) the decrease of the strain energy[36] caused by the transition of the six-membered ring from the *boat* to the *chair* conformation and (ii) the above bonding H···H interaction. The $C(3)H_2$ group should be the one least affected by the decrease in strain energy, since it remains in the ring with the "chair" conformation. Thus, the H···H bonding is the main cause of $\Delta E = -1.6$ kcal/mol for this group. As the **CC-cc** conformer is characterized by the C_{2v} point group symmetry, the gain in energy due to this bonding for the $C(7)H_2$ group is the same, resulting in the total lowering of the energy of the system due to the H···H interaction by 3.2 kcal/mol. This value is almost equal to the E_{int} estimated by means of CEML correlation for the H···H interaction (2.9 kcal/mol) (see Table 2). It should also be noted that without this stabilizing contribution the *cb* conformation of bicyclo[3.3.1]nonane would be the preferred one, having energy 0.5 kcal/mol lower than the *cc* conformation (see Table 3). This was also the case of 7α-phenyl-3-borabicyclo-[3.3.1]nonane with the stabilizing contribution of the B···π interaction (B···C is 2.908(1) Å, $\rho(\mathbf{r}) = 0.074(4)$ e·Å^{-3}, $\nabla^2\rho(\mathbf{r}) = 0.747(5)$ e·Å^{-5}) being 1.8 kcal/mol.[34,35] As we can see, despite the claims in the literature that the H···H attractive interactions "do not exist",[52] the bicyclo[3.3.1]nonane is one more example of a system where they play a significant stabilizing role.

Assuming that the 3,7 bonding interaction results in ΔE for the atoms in both the positions 3 and 7 by $0.5E_{int}$ each, we can calculate the destabilizing contribution of the lone pairs of the sulfur atoms approaching each other in **SC** and **SN** as $\Delta E(S(3)) + 0.5(E_{int})_{S\cdots S} = 2.1 + 1.3 = 3.4$ kcal/mol for each sulfur atom. This is the direct estimation of how much the "hockey sticks" effect costs the system. The fact that the **SC** conformers differ by less than the expected $3.4 \times 2 - 2.5 = 4.3$ kcal/mol (the value calculated summing the contributions of the "hockey sticks" effect to the bicyclo[3.3.1]nonane's difference between conformers) can be explained by lesser strain in **SC-cc** in comparison to **CC-cc** leading to the higher gain in energy as a result of the *cc*−*cb* transition. The stabilization of the *cc* conformation in **DTDABCN** is in turn caused by two LP−N−C−S SEIs contributing $((E(cc) - E(cb))_{SN} - (E(cc) - E(cb))_{SC})/2 = (-3.80 - 1.43)/2 = -2.6$ kcal/mol each.

CONCLUSIONS

With the investigation of the conformers of the bicyclo-[3.3.1]nonanes by means of the topological analysis of the $\rho(\mathbf{r})$ and $-\nabla^2\rho(\mathbf{r})$ functions and the comparison of the variations in atomic energies, a novel interpretation of the difference in energy observed between the conformers of both the unsubstituted bicyclo[3.3.1]nonane and its 3,7-dithia derivatives has emerged. The chosen approach allowed separating the exact contributions of different factors underlying the conformational preferences. We have shown that the preference to the chair−chair conformation of the unsubstituted bicyclo[3.3.1]nonane results only from the H···H interaction between CH_2 groups at the positions 3 and 7 causing the estimated gain in energy of 3.2 kcal/mol in favor of the *cc* conformer. At the same time, the "hockey sticks" effect in 3,7-dithia derivatives of bicyclo-[3.3.1]nonane, which states that the approach of sulfur atoms at the positions 3 and 7 destabilizes the system, also received the explanation. Despite the presence of the attractive S···S interaction estimated as worth 2.9 kcal/mol both in a crystal and in an isolated state, the close contact of sulfur atoms causes them to lose the electron population and thus induces the rise in the energy of the system by approximately 6.8 kcal/mol, resulting in the preference to the *cb* conformation in the 3,7-dithia derivatives. The preference to the *cc* conformation of 3,7-dithia-1,5-diazabicyclo[3.3.1]nonane is provided by two additional LP−N−C−S stereoelectronic interactions (as compared to the *cb* conformation), contributing 2.6 kcal/mol each to the stabilization of the *cc* conformer.

dx.doi.org/10.1021/jp203730b |*J. Phys. Chem. A* XXXX, XXX, 000–000

EXPERIMENTAL SECTION

The crystals of **DTDABCN** were grown by slow cooling of saturated ethanol solution. The high-resolution X-ray diffraction data were obtained on a SMART 1000 CCD diffractometer (graphite monochromated Mo Kα radiation, λ = 0.71073 Å) equipped with an Oxford Cryo-Flex low temperature device. Intensities of 13087 reflections were collected at 120 K by series of ω scans within the 2θ range of 6−100°. Data reduction was performed with the SAINT program, semiempirical absorption correction was applied with the SADABS program using the intensity data of the equivalent reflections.

The structure was solved by direct method and refined first in anisotropic−isotropic approximation using the SHELX package.[53] Then we performed the multipole refinement within the Hansen−Coppens formalism in order to obtain the experimental $\rho(\mathbf{r})$ function. The multipole refinement and data analysis were performed with the XD2006 package.[54]

Coordinates for hydrogen atoms were derived from C−H distances of the ab initio optimized structure. Atomic coordinates and anisotropic displacement parameters for heavy atoms were first refined against high-order reflections ($\sin(\theta/\lambda) > 0.7$). Then multipole occupancies, k', and monopole population were sequentially refined using the low-order data ($\sin(\theta/\lambda) < 0.7$). The multipole model was expanded to the octupole level ($l = 3$) for the heavy atoms and the dipole level ($l = 1$) for hydrogen atoms, the multipole occupancies of the atom C(9) was restrained according to the C_2 site symmetry. The refinement of the hexadecapole occupancies ($l = 4$) for the S atom led to the deterioration of charge distribution pattern and did not affect the convergence criteria and therefore was omitted. The whole procedure was repeated to the full convergence of parameters. Finally, k'' and coordinates were refined using all data. The results of the multipole refinement can be found in Tables S17−S21 in the Supporting Information.

The refinement converged to $R = 0.0267$, wR = 0.0276, GOF = 0.972 for 2306 reflections with $I > 3\sigma(I)$. The Hirshfeld rigid body test[55] confirmed that the values of U_{ij} are reliable, with a maximum (8×10^{-4} Å^2) for the S3−C4 bond. Subsequent topological analysis of the charge density distribution was performed using the WinXPRO package.[56]

The potential energy density $v(\mathbf{r})$ in a crystal was evaluated through the Kirzhnits's approximation[57] for the kinetic energy density function $g(\mathbf{r})$. Accordingly, the $g(\mathbf{r})$ function is described by the equation

$$g(\mathbf{r}) = (3/10)(3\pi^2)^{2/3}[\rho(\mathbf{r})]^{5/3} + (1/72)|\nabla\rho(\mathbf{r})|^2/\rho(\mathbf{r}) + 1/6\nabla^2\rho(\mathbf{r})$$

in conjunction with the local virial theorem ($2g(\mathbf{r}) + v(\mathbf{r}) = 1/4\nabla^2\rho(\mathbf{r})$) leading to the expression for $v(\mathbf{r})$[1] and, thus, for the electron energy density $h_e(\mathbf{r})$.

COMPUTATIONAL DETAILS

The calculations for the bicyclic structures were performed at the MP2(full)/6-311++G**//MP2(full)/6-311++G** level of theory using the Gaussian 03 package[58] with "very tight" convergence criteria. The calculation of frequencies for all the conformers ensured that they corresponded to local energetic minima. The QTAIM analysis of the resulted wave functions was performed using the AIMAll program package.[59] The optimized coordinates for the calculated molecules as well as the results of atomic basins integration can be found in Tables S3−S15 in the Supporting Information.

Table 6. Homodesmotic Strain and Conformational Energy Values in Cyclohexane and Thiane Molecules, kcal/mol

X	$E_s(b)$	$E_s(c)$	$E_{conf}(b) = E_s(b) - E_s(c)$
CH_2	10.20	2.63	7.57
S	8.19	1.06	7.13

The strain energy evaluation for the cyclohexane and thiane were performed at the MP2/aug-cc-pVDZ[60] level with harmonic zero-point energy corrections (after the geometry optimization) using version 7.1.G of the Firefly quantum chemistry package[61,62] (which in turn is originally based on the GAMESS(US) program[63]). The correlation-consistent basis set was retrieved from the EMSL Basis Set Exchange portal.[64,65]

The strain energy values E_s (Table 6) were obtained for both the most stable chair conformer (c) and the boat transition state conformation (b), their difference being the conformational energy of the boat (relative to the chair).

X = CH_2, S

The calculations utilized the following bond separation reaction scheme, when both the number of atoms of various types and the number of bonds of different types are conserved. This scheme belongs to the class of the so-called "hyperhomodesmotic" reactions, which make the molecular strain calculation results reliable even with the modest theory levels.[66]

These results reveal the slightly increased strain for the cyclohexane molecule compared to the thiane in both these conformations resulted in the decrease in the boat conformational energy value for the latter compound.

ASSOCIATED CONTENT

Supporting Information. A CIF file, the summary of critical points in the crystal, the optimized molecular geometries for the conformers in isolated state, results of the atomic basin integration, and the details of the multipole refinement. This information is available free of charge via the Internet at http://pubs.acs.org/.

AUTHOR INFORMATION

Corresponding Author

*E-mail: kostya@xrlab.ineos.ac.ru.

ACKNOWLEDGMENT

This work was supported by the Russian Foundation for Basic Research (Project No. 10-03-00578) and by the Council on Grants

at the President of the Russian Federation (Program for State Support of Young Doctors of Science, Project MD-237.2010.3).

REFERENCES

(1) Bader, R. F. W. *Atoms in Molecules: A Quantum Theory*; Oxford University Press, New York, 1994.
(2) Bader, R. F. W.; Bayles, D. *J. Phys. Chem. A* **2000**, *104*, 5579–5589.
(3) Cortés-Guzmán, F.; Bader, R. F. W. *Chem. Phys. Lett.* **2003**, *379*, 183–192.
(4) Bader, R. F. W. *J. Phys. Chem. A* **2008**, *112*, 13717–13728.
(5) Wiberg, K. B.; Bader, R. F. W.; Lau, C. D. H. *J. Am. Chem. Soc.* **1987**, *109*, 1001–1012.
(6) Koch, U.; Popelier, P. L. A. *J. Phys. Chem.* **1995**, *99*, 9747–9754.
(7) Matta, C. F.; Hernández-Trujillo, J.; Tang, T.-H.; Bader, R. F. W. *Chem.—Eur. J.* **2003**, *9*, 1940–1951.
(8) Popelier, P. L. A. *J. Phys. Chem. A* **1998**, *102*, 1873–1878.
(9) Eskandari, K.; Vila, A.; Mosquera, R. A. *J. Phys. Chem. A* **2007**, *111*, 8491–8499.
(10) Mandado, M.; Mosquera, R. A.; Alsenoy, C. V. *Tetrahedron* **2006**, *62*, 4243–4252.
(11) Vila, A.; Mosquera, R. A. *J. Comput. Chem.* **2007**, *28*, 1516–1530.
(12) Bushmarinov, I. S.; Antipin, M. Yu.; Akhmetova, V. R.; Nadyrgulova, G. R.; Lyssenko, K. A. *J. Phys. Chem. A* **2008**, *112*, 5017–5023.
(13) Berestovitskaya, V. M.; Makarenko, S. V.; Bushmarinov, I. S.; Lyssenko, K. A.; Smirnov, A. S.; Stukan', E. V. *Russ. Chem. Bull.* **2010**, *58*, 1023–1033.
(14) Kirby, A. J. *The anomeric effect and related stereoelectronic effects at oxygen*; Springer: Berlin, 1983.
(15) Bader, R. F. W. *J. Phys. Chem. A* **1998**, *102*, 7314–7323.
(16) Pendás, A. M.; Francisco, E.; Blanco, M. A.; Gatti, C. *Chem.—Eur. J.* **2007**, *13*, 9362–9371.
(17) Espinosa, E.; Molins, E.; Lecomte, C. *Chem. Phys. Lett.* **1998**, *285*, 170–173.
(18) Espinosa, E.; Lecomte, C.; Molins, E. *Chem. Phys. Lett.* **1999**, *300*, 745–748.
(19) Espinosa, E.; Alkorta, I.; Rozas, I.; Elguero, J.; Molins, E. *Chem. Phys. Lett.* **2001**, *336*, 457–461.
(20) Espinosa, E.; Alkorta, I.; Elguero, J.; Molins, E. *J. Chem. Phys.* **2002**, *117*, 5529.
(21) Espinosa, E.; Molins, E. *J. Chem. Phys.* **2000**, *113*, 5686.
(22) Lyssenko, K. A.; Nelyubina, Yu. V.; Kostyanovsky, R. G.; Antipin, M. Yu. *ChemPhysChem* **2006**, *7*, 2453–2455.
(23) Lyssenko, K. A.; Korlyukov, A. A.; Golovanov, D. G.; Ketkov, S. Y.; Antipin, M. Yu. *J. Phys. Chem. A* **2006**, *110*, 6545–6551.
(24) Lyssenko, K. A.; Korlyukov, A. A.; Antipin, M. Yu. *Mendeleev Commun.* **2005**, *15*, 90–92.
(25) Glukhov, I. V.; Lyssenko, K. A.; Korlyukov, A. A.; Antipin, M. Yu. *Faraday Discuss.* **2007**, *135*, 203–215.
(26) Nelyubina, Yu. V.; Glukhov, I. V.; Antipin, M. Yu.; Lyssenko, K. A. *Chem. Commun.* **2010**, *46*, 3469.
(27) Sobczyk, L.; Grabowski, S. J.; Krygowski, T. M. *Chem. Rev.* **2005**, *105*, 3513–3560.
(28) Pidko, E. A.; van Santen, R. A. *ChemPhysChem* **2006**, *7*, 1657–1660.
(29) Pidko, E. A.; Xu, J.; Mojet, B. L.; Lefferts, L.; Subbotina, I. R.; Kazansky, V. B.; van Santen, R. A. *J. Phys. Chem. B* **2006**, *110*, 22618–22627.
(30) Korlyukov, A. A.; Lyssenko, K. A.; Antipin, M. Yu.; Grebneva, E. A.; Albanov, A. I.; Trofimova, O. M.; Zel'bst, E. A.; Voronkov, M. G. *J. Organomet. Chem.* **2009**, *694*, 607–615.
(31) Puntus, L. N.; Lyssenko, K. A.; Antipin, M. Yu.; Bünzli, J.-C. G. *Inorg. Chem.* **2008**, *47*, 11095–11107.
(32) Borissova, A. O.; Korlyukov, A. A.; Antipin, M. Yu.; Lyssenko, K. A. *J. Phys. Chem. A* **2008**, *112*, 11519–11522.
(33) Nelyubina, Yu. V.; Dalinger, I. L.; Lyssenko, K. A. *Angew. Chem., Int. Ed.* **2011**, *50*, 2892–2894.
(34) Gurskii, M. E.; Lyssenko, K. A.; Karionova, A. L.; Belyakov, P. A.; Potapova, T. V.; Antipin, M. Yu.; Bubnov, Yu. N. *Russ. Chem. Bull.* **2004**, *53*, 1963–1977.
(35) Lyssenko, K. A.; Antipin, M. Yu.; Gurskii, M. E.; Bubnov, Yu. N.; Karionova, A. L.; Boese, R. *Chem. Phys. Lett.* **2004**, *384*, 40–44.
(36) Zefirov, N. S.; Palyulin, V. A. In *Topics in Stereochemistry*; John Wiley & Sons, Inc.: Hoboken, NJ, 1991; Vol. 20, pp 171−230.
(37) Choo, J.; Kim, S.; Joo, H.; Kwon, Y. *J. Mol. Struct. THEOCHEM* **2002**, *619*, 113–120.
(38) Zefirov, N. S. *Tetrahedron* **1977**, *33*, 3192.
(39) Gustaffson, R. *Int. J. Sulfur Chem., Part A* **1971**, *1*, 233–241.
(40) Gleiter, R.; Kobayashi, M.; Zefirov, N. S.; Palyulin, V. A. *Proc. Natl. Acad. Sci. USSR* **1977**, *235*, 347–350.
(41) Cadenas-Pliego, G.; Contreras, R.; Flores-Parra, A.; Daran, J. C.; Halut, S. *Phosphorus, Sulfur Silicon Relat. Elem.* **1993**, *84*, 9.
(42) Potekhin, K. A.; Kurkutova, E. N. *Proc. Natl. Acad. Sci. USSR* **1977**, 813.
(43) Gleiter, R.; Zefirov, N. S.; Palyulin, V. A.; Potekhin, K. A.; Kurkutova, E. N.; Struchkov, Y. T.; Antipin, M. Yu. *Zh. Org. Khim.* **1978**, *14*, 1630–1631.
(44) Allen, F. H.; Watson, D. G.; Brammer, L.; Orpen, A. G.; Taylor, R. In *International Tables for Crystallography*; Prince, E., Ed.; International Union of Crystallography: Chester, England, 2006; Vol. C, pp 790−811.
(45) Cremer, D.; Kraka, E. *Croat. Chem. Acta* **1984**, *57*, 1259–1281.
(46) McCormack, K. L.; Mallinson, P. R.; Webster, B. C.; Yufit, D. S. *Faraday Trans.* **1996**, *92*, 1709.
(47) Bukalov, S. S.; Leites, L. A.; Lyssenko, K. A.; Aysin, R. R.; Korlyukov, A. A.; Zubavichus, J. V.; Chernichenko, K. Y.; Balenkova, E. S.; Nenajdenko, V. G.; Antipin, M. Yu. *J. Phys. Chem. A* **2008**, *112*, 10949–10961.
(48) Scherer, W.; Spiegler, M.; Pedersen, B.; Tafipolsky, M.; Hieringer, W.; Reinhard, B.; Downs, A. J.; McGrady, G. S. *Chem. Commun.* **2000**, 635–636.
(49) Nelyubina, Yu. V.; Antipin, M. Yu.; Lyssenko, K. A. *J. Phys. Chem. A* **2007**, *111*, 1091–1095.
(50) Mastryukov, V. S.; Popik, M. V.; Dorofeeva, O. V.; Golubinskii, A. V.; Vilkov, L. V.; Belikova, N. A.; Allinger, N. L. *J. Am. Chem. Soc.* **1981**, *103*, 1333–1337.
(51) Wiberg, K. B.; Bader, R. F. W.; Lau, C. D. H. *J. Am. Chem. Soc.* **1987**, *109*, 985–1001.
(52) Poater, J.; Solà, M.; Bickelhaupt, F. M. *Chem.—Eur. J.* **2006**, *12*, 2889–2895.
(53) Sheldrick, G. *Acta Crystallogr., Sect. A* **2008**, *64*, 112–122.
(54) Koritsansky, T. S.; Howard, S. T.; Richter, T.; Macchi, P.; Volkov, A.; Gatti, C.; Mallinson, P. R.; Farrugia, L. J.; Su, Z.; Hansen, N. K. *XD—A Computer program package for multipole refinement and Topological Analysis of charge densities from diffraction data*, 2003.
(55) Hirshfeld, F. L. *Theor. Chim. Acta* **1977**, *44*, 129–138.
(56) Stash, A.; Tsirelson, V. *J. Appl. Crystallogr.* **2002**, *35*, 371–373.
(57) Kirzhnits, D. A. *Sov. Phys. JETP* **1957**, *5*, 64.
(58) Frisch, M. J.; Trucks, G. W.; Schlegel, H. B.; Scuseria, G. E.; Robb, M. A.; Cheeseman, J. R.; Montgomery, J.; Vreven, T.; Kudin, K. N.; Burant, J. C. et al. *Gaussian 03, Revision E.01*; Gaussian, Inc.: Wallingford, CT, 2004.
(59) Keith, T. A. *AIMAll (Version 09.02.01, aim.tkgristmill.com)*, 2009.
(60) Dunning, T. H. *J. Chem. Phys.* **1989**, *90*, 1007.
(61) Granovsky, A. *Firefly version 7.1.G*, http://classic.chem.msu.su/.
(62) Granovsky, A. A. *J. Chem. Phys.* **2011**, *134*, 214113.
(63) Schmidt, M. W.; Baldridge, K. K.; Boatz, J. A.; Elbert, S. T.; Gordon, M. S.; Jensen, J. H.; Koseki, S.; Matsunaga, N.; Nguyen, K. A.; Su, S.; et al. *J. Comput. Chem.* **1993**, *14*, 1347–1363.
(64) EMSL Basis Set Exchange https://bse.pnl.gov/bse/portal (accessed Aug 5, 2011).
(65) Schuchardt, K. L.; Didier, B. T.; Elsethagen, T.; Sun, L.; Gurumoorthi, V.; Chase, J.; Li, J.; Windus, T. L. *J. Chem. Inf. Model.* **2007**, *47*, 1045–1052.
(66) Wheeler, S. E.; Houk, K. N.; Schleyer, P. v. R.; Allen, W. D. *J. Am. Chem. Soc.* **2009**, *131*, 2547–2560.